Nanostructure, Composition and Luminescence Properties of Porous Silicon Layer Subjected to Various Surface Treatments

K. Shigyo*, K. Azumi, and M. Seo

Graduate School of Engineering, Hokkaido University
North 13, West 8, Kita-ku, Sapporo, 060, Japan
Tel/Fax : 011 - 706 - 6737
E-mail : shigyo@icnet.hokudai.ac.jp

(Received: Jan. 30, 1997 Accepted: Mar. 7, 1997)

Abstract

A porous silicon Layer (PSL) was prepared on p-type Silicon (100) wafer with electrochemical etching in HF aqueous solution. The PSL was subjected to the surface treatments (anodic oxidation, dip into HF aqueous solution, dry oxidation, hydrothermal oxidation) to examine the correlation between nanostructure, crystallinity, composition and visible luminescence properties of PSL. The nanostructure and crystallinity of PSL were investigated by TEM observation and the surface characterization were performed by using FT-IR and XPS. The spectra of photoluminescence (PL) were measured to examine the visible luminescence properties. The high resolution TEM images and TED patterns showed that the PSL as prepared with electrochemical etching consists of Si particles with a diameter of 2nm – 3nm and has a mosaic structure of crystal and amorphous. The PSL subjected to anodic oxidation or hydrothermal oxidation has an amorphous structure. It is found that the visible PL intensity increases with decreasing concentration of silicon hydrides (SiH_x) only for the PSL prepared under different electrochemical etching conditions. The PL intensity of PSL was enhanced significantly by HF dip treatment after anodic oxidation or by hydrothermal oxidation. No correlation between nanostructure, crystallinity, composition (SiH_x, elemental Si and SiO_2) and PL intensity was observed for the PSL subjected to the surface treatments. The reason for no correlation was explained in terms of the difference in information depth between FT-IR, XPS and PL emission or in depth-distribution between each constituent (SiH_x, elemental Si and SiO_2) and PL center.

1. Introduction

It is known that a porous silicon layer (PSL) prepared on silicon with electrochemical etching emits a visible luminescence[1, 2]. Thus, PSL is promissing as new luminescence devices. The quantum confinement effect has been proposed for the visible luminescence of PSL[3, 4] because the PSL consists of silicon particles with a diameter of several nanometers. On the other hand, it has been pointed out that the surface silicon compounds such as siloxene ($Si_6O_3H_6$) play a vital role in visible luminescence[5, 6]. In our previous study[7 - 9], it has been reported that the quantum confinement effect is operative in the visible luminescence from the PSL, whereas the luminescence intensity is influenced by the amount of silicon hydrides (SiH_x) in the PSL. Vial et al.[10] reported that the anodic oxidation of PSL in 0.1 M KNO_3 aqueous solution enhanced the PL intensity with shift of peak toward short wavelength. On the other hand, the PL peak shifted toward long wavelength by dipping the PSL into HF solution after anodic oxidation[11]. Kanemitsu et al.[12] found that the PSL subjected to dry oxidation at temperatures above 800°C emitted a strong blue PL. The blue shift in PL was also observed from the PSL subjected to hydrothermal oxidation in boiling water[13]. The above results indicated that the surface treatments of PSL influences sensitively the PL intensity and spectra. The surface treatments of PSL would change the nanostructure, crystallinity and composition of PSL which control the luminescence properties. However, there are few studies of PSL correlating the nanostructure, crystallinity and composition with the luminescence properties. In this study, the correlation between nanostructure, crystallinity, composition, and luminescence properties was investigated for the PSL subjected to the typical surface treatments[10 - 13] which were chosen from literatures.

2. Experimental

2.1 PSL Preparation

Single crystal p-type silicon (100) wafer with specific resistivity of ρ = 1kΩ m was employed for this experiments. The ohmic contact with

back side of the wafer was taken with evaporation of aluminum. The mirror-finishing surface of the front side was covered with dielectric organic film except for the area of 1cm × 1cm subjected to electrochemical etching. The electrochemical etching for preparation of PSL was performed under different galvanostatic conditions of $i = 25Am^{-2}$ – $2kAm^{-2}$ for 23s – 1.8ks in 5.8wt% – 35wt% HF aqueous solutions. The total electric charge passed for electrochemical etching was kept constant ($45kCm^{-2}$). The PSL prepared was subjected to the following surface treatments :

a) anodic oxidation in 0.1 M KNO_3 ethylene glycol solution under galvanostatic condition of $i = 10Am^{-2}$ for 1ks

b) dip into 0.5wt% HF aqueous solution for 10s after the anodic oxidation

c) dry oxidation at 800°C for 30s in air

d) hydrothermal oxidation for 600s in boiling water

2.2 Luminescence properties, nanostructure and surface characterization of PSL

The photoluminescence (PL) spectra were measured by using a fluorometer (HITACHI F3010) at an excitation wavelength of 350nm.

The surface and cross sectional morphologies of PSL were observed with a field emission scanning electron microscope (FE-SEM). The PSL was detached from the Si substrate with tweezers as flakes which were sprinkled over the copper mesh covered with collodion film for TEM observation. The nanostructure and crystallinity of PSL flakes were observed by using transmission electron microscope (TEM) and electron diffraction (TED), respectively.

The surface chemical species of PSL were identified by using a FT-IR spectrometer (JASCO FT-IR 8000) equipped with a TGS detector. The FT-IR spectra in the wavenumber range of $4600cm^{-1}$ – $400cm^{-1}$ were measured by signal averaging of 150 scans at a resolution of $4cm^{-1}$.

The oxidation states of Si in PSL were evaluated by XPS analysis of Si 2p binding energy. A VG ESCALAB Mark II spectrometer was employed for the analysis. A AlKα X-ray was used with 10kV anode potential and 5mA emission current. The pass energies in the hemispherical analyzer were 50eV for survey scans and 20eV for high resolution narrow scans. The spectra energy scale was calibrated with C 1s at 284.6eV.

3. Results and Discussion

3.1 PSL prepared with different electrochemical etching conditions

In **Fig. 1**, the thickness of PSL was plotted versus HF concentration and current density employed for electrochemical etching. The thickness (the mean value of three different points of PSL cross section) was determined by FE-SEM observation of PSL cross section. It is seen that the PSL thickness is almost constant (4μm) irrespective of HF concentration and current density under a constant electric charge passed ($45kCm^{-2}$).

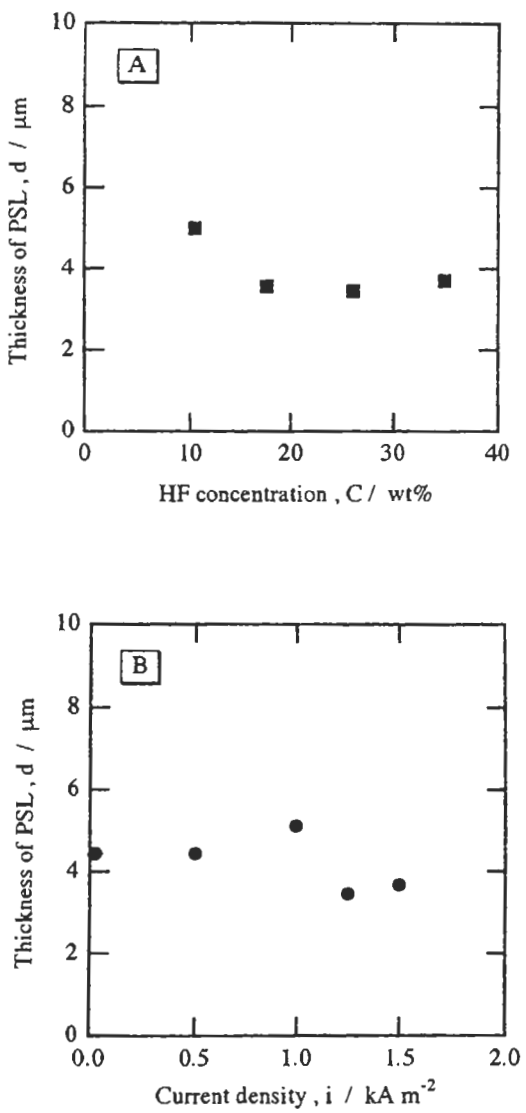

Fig. 1 Thickness of PSL versus HF concentration (A) and current density employed for electrochemical etching (B)
(The electric charge, $Q = 45kCm^{-2}$)

Fig. 2 shows the typical PL spectrum (**Fig. 2A**) and FT-IR spectrum (**Fig. 2B**) of PSL. The preparation conditions are described in the figure caption. In **Fig. 2**, the PL has a broad spectrum with a peak at a wavelength of 645nm. In **Fig. 2B**, several absorbance peaks are observed. According to several researchers[14 -16], the absorbance peaks in the wavenumber domains of $2150cm^{-1} - 2050cm^{-1}$, $950cm^{-1} - 900cm^{-1}$, and $750cm^{-1} - 550cm^{-1}$ are assigned to stretching, scissors, and bending of Si hydrides (SiH_x), respectively. On the other hand, the absorbance peak in the range of $1150cm^{-1} - 1000cm^{-1}$ is assigned to the bond of silicon and oxygen (Si-O). The peak of SiH_x stretching is conventionally employed for quantification of SiH_x [17, 18]. Thus, the amount of SiH_x present in the PSL may be relatively determined from the peak height of SiH_x stretching.

The FT-IR absorbance peak height of SiH_x stretching and Si-O bond, and logarithm of PL peak intensity are plotted versus HF concentration in **Fig. 3A** and current density in **Fig. 3B**. It is seen that the PL peak intensity increases with decreasing HF concentration or increasing current density. **Fig. 3A** and **Fig. 3B** also demonstrate that the PL peak intensity decreases with increasing absorbance of SiH_x. On the other hand, the absorbance of Si-O bond is very small or almost zero for all the PSL prepared in this conditions. The wavelength at the peak of PL spectra was almost kept constant at around 650nm.

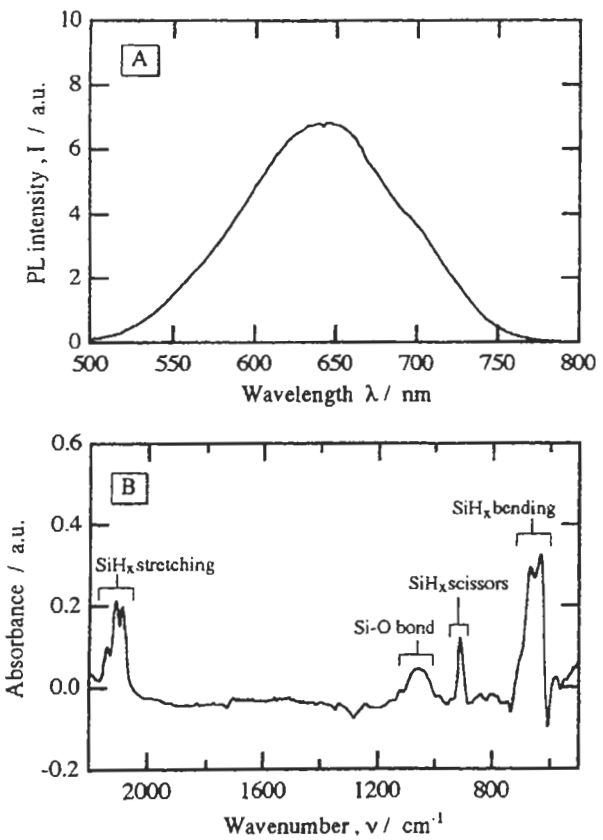

Fig. 2 Typical PL spectrum and FT-IR spectrum of PSL
The PSL was prepared with electrochemical etching ($25A\ m^{-2}$, 1.8ks) in 10.4wt% HF solution.

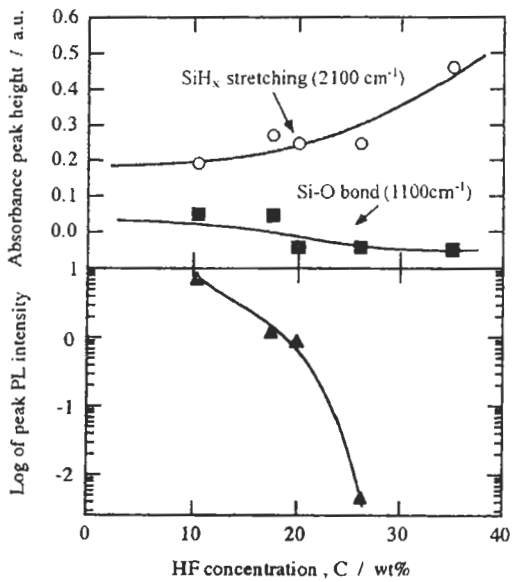

Fig. 3A FT-IR absorbance of SiH_x stretching and Si-O bond, and logarithm of PL peak intensity as a function of HF concentration
The PSL was prepared with electrochemical etching ($25Am^{-2}$, 1.8ks).

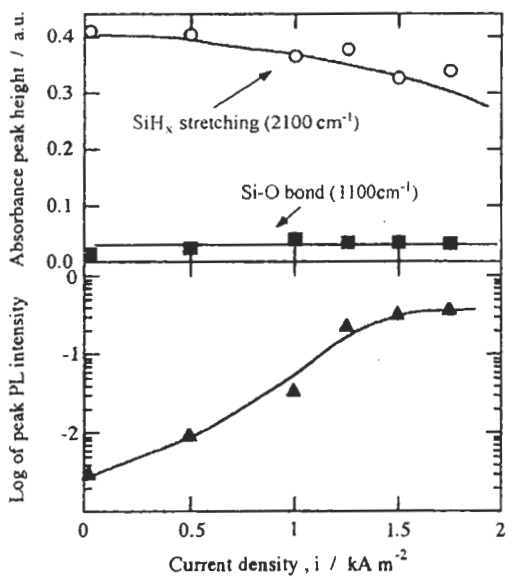

Fig. 3B FT-IR absorbance of SiH_x stretching and Si-O bond, and logarithm of PL peak intensity as a function of current density
The PSL was prepared in 26wt% HF solution and the total electric charge was kept constant ($45kCm^{-2}$).

Fig. 4 shows the TEM images and TED patterns of PSL prepared under different HF concentrations (**Fig. 4A** and **Fig. 4C**) and current densities (**Fig. 4B** and **Fig. 4D**). The TEM images indicate that the PSL consists of Si particles with a diameter of 2nm – 3nm and that the nanostructure of PSL does not sensitively depend on the electrochemical etching conditions. The quantum confinement effect [19,20] would be operative in the PSL because the Si particles with a diameter of 2nm – 3nm have a band gap energy extended to 2eV – 1.6eV, which is consistent with the band gap energy (1.9eV) expected from wavelength (650nm) at the PL peak. The TED patterns with diffuse spots and halo rings suggest that the PSL consists of a mosaic structure of crystal and amorphous. It is generally accepted that hydrogen atoms terminate Si dangling bonds which act as a nonradiation center [21, 22] and the SiH_x formation would improve the luminescence efficiency. The present results, however, are not consistent with the above speculation because the PL intensity decreases with increasing the amount of SiH_x in the PSL. In the case of high concentration of SiH_x in the PSL, Si dangling bonds are not only diminished due to hydrogen termination but also the excess hydrogen atoms may form many surface states in the band gap of Si nanoparticles like an amorphous Si to lower the luminescence efficiency due to the recombination of electrons in the conduction band with positive holes in the valence band through the surface states.

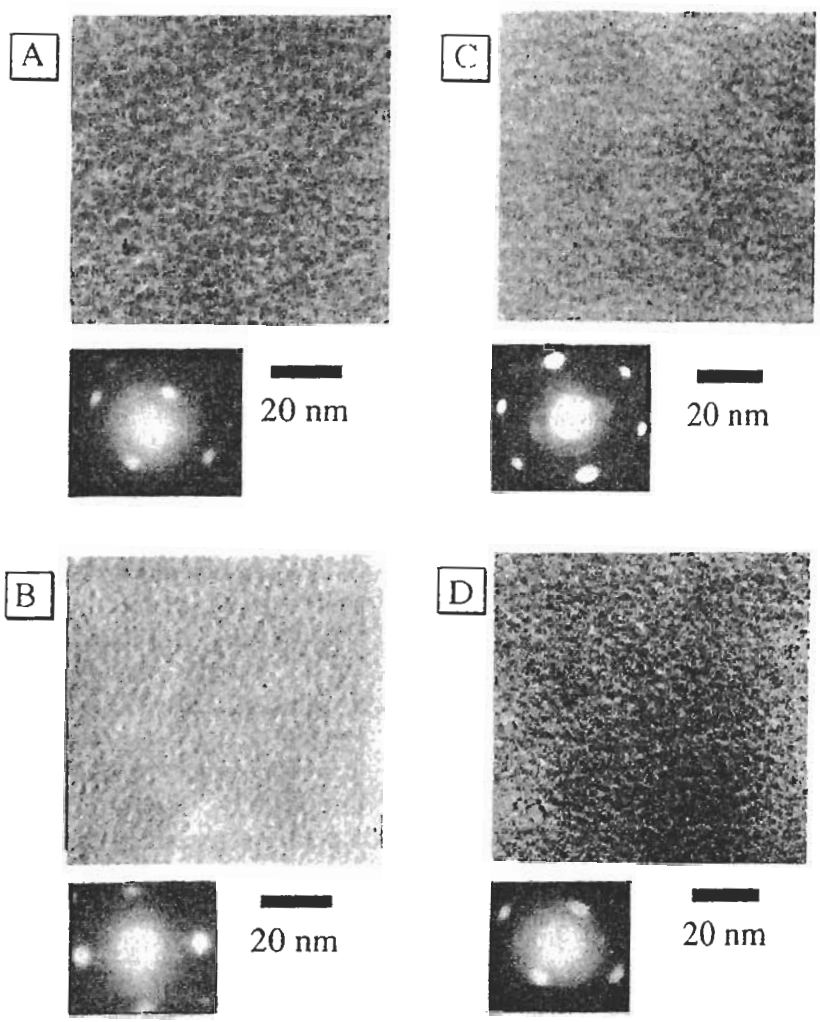

Fig. 4 TEM images and TED patterns of PSL prepared with the following electrochemical etching conditions
A: 10.4wt% HF, i = 25Am^{-2}, t = 1.8ks
B: 35wt% HF, i = 25Am^{-2}, t = 1.8ks
C: 26wt% HF, i = 25Am^{-2}, t = 1.8ks
D: 26wt% HF, i = 1.75kAm^{-2}, t = 43s

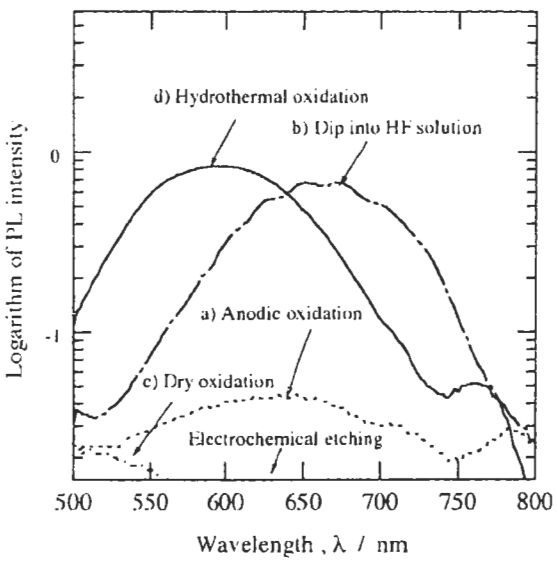

Fig. 5 PL spectra of PSL subjected to the following surface treatments
a) Anodic oxidation for 1ks in 0.1 M KNO_3 ethylene glycol solution under galvanostatic condition of $i = 10Am^{-2}$
b) Dip into 0.5wt% HF aqueous solution for 10 s after anodic oxidation
c) Dry oxidation at 800°C for 30s in air
d) Hydrothermal oxidation for 600s in boiling water
The reference PSL was prepared with electrochemical etching ($25Acm^{-2}$, 1.8ks) in 35wt% HF solution.

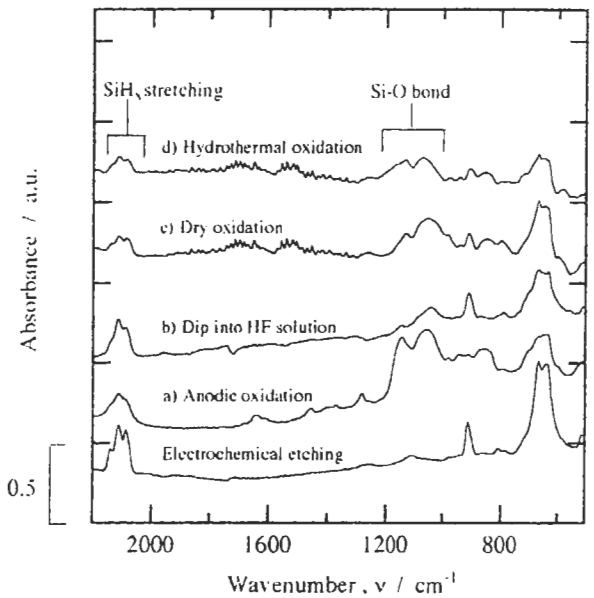

Fig. 6 FT-IR spectra of PSL subjected to the following surface treatments
a) Anodic oxidation for 1ks in 0.1 M KNO3 ethylene glycol solution under galvanostatic condition of $i = 10Am^{-2}$
b) Dip into 0.5wt% HF aqueous solution for 10s after anodic oxidation
c) Dry oxidation at 800°C for 30s in air
d) Hydrothermal oxidation for 600s in boiling water
The reference PSL was prepared with electrochemical etching ($25Am^{-2}$, 1.8ks) in 35wt% HF solution.

3.2 PSL subjected to the surface treatments

The PSL prepared with electrochemical etching at $25Am^{-2}$ for 1.8ks in 35wt% HF solution was employed as a reference sample subjected to the surface treatments. As shown in **Fig. 3A**, the reference PSL includes the high concentration of SiH_x and emits no visible luminescence.

Fig. 5 shows the PL spectra of PSL subjected to the surface treatments a), b), c), and d). It is emphasized that the surface treatments b) and d) enhance significantly the PL intensity. The difference in wavelength of the PL peak between the PSL subjected to the surface treatments b) and c) may result from the difference in diameter of Si nanoparticle. On the other hand, a weak or only slight PL is emitted from the PSL subjected to the surface treatment a) or c). The strong blue PL reported by Kanemitsu et al.[12] or Hou et al.[13] was not observed from the PSL subjected to the surface treatments c) and d). This discrepancy between the present results and literatures[12, 13] may be ascribed to the difference in preparation condition of the reference PSL.

Fig. 6 shows the FT-IR spectra of PSL subjected to the surface treatments a) - d). It is seen from comparison of **Fig. 5** and **Fig. 6** that the decrease in SiH_x concentration does not always correspond to the increase in PL intensity. Moreover, there is no correlation between Si-O bond and PL intensity.

Fig. 7 shows the TEM images and TED patterns of the PSL subjected to the surface treatments a) - d). The PSL subjected to the surface treatments except for d) consists of Si nanoparticles. On the other hand, the structure of PSL subjected to the surface treatment d) is not clearly observed from the TEM images. The crystallinity of PSL subjected to the surface treatments a) or d) is amorphous, whereas the PSL subjected to the surface treatments b) or c) has a mosaic structure of crystal and amorphous. The amorphous structure may be associated with a dielectric hydrous oxide formed due to the surface treatments a) or d).

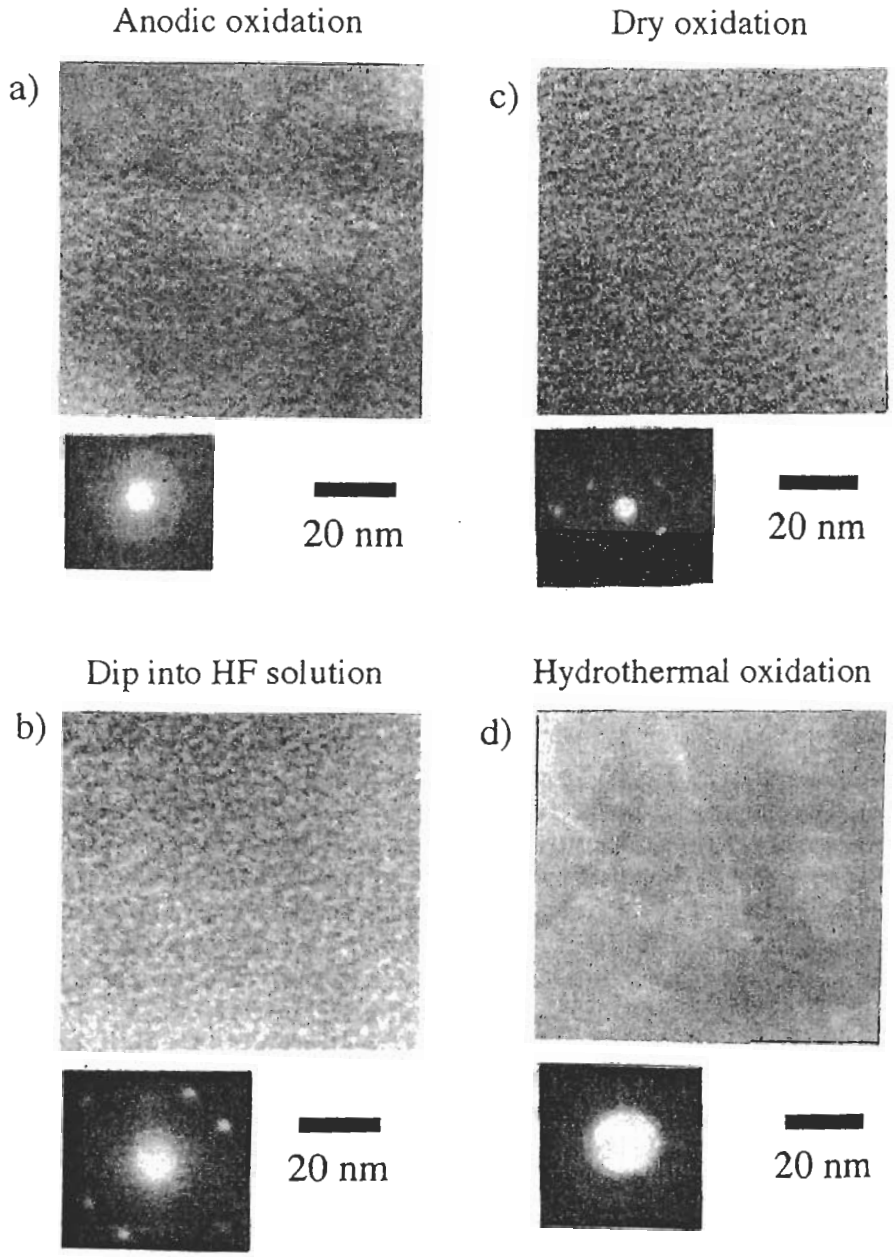

Fig. 7 TEM images and TED patterns of PSL subjected to the following surface treatments
a) Anodic oxidation for 1ks in 0.1 M KNO_3 ethylene glycol solution under galvanostatic condition of $i = 10Am^{-2}$
b) Dip into 0.5wt% HF aqueous solution for 10s after anodic oxidation
c) Dry oxidation at 800°C for 30s in air
d) Hydrothermal oxidation for 600s in boiling water
The reference PSL was prepared with electrochemical etching ($25Acm^{-2}$, 1.8ks) in 35wt% HF solution.

Fig. 8 shows the results of XPS survey scan and high resolution narrow scan of Si 2p (inset) for the PSL as prepared with electrochemical etching. There are five peaks at the binding energy of 100eV, 150eV, 285eV, 530eV, which are assigned to Si 2p, Si 2s, C 1s, O 1s, respectively. The Si 2p spectrum in the high resolution narrow scan indicates that two different states of Si are present in the PSL. Thus, the Si 2p spectra were deconvoluted into two peaks of low binding energy (peak 1) and high binding energy (peak 2). The binding energy of peak 1 is close to that of elemental Si (99.4eV) in the literature[23]. It seems difficult to discriminate between Si in SiH_x and elemental Si from the Si 2p spectrum because any difference in binding energy between them has not been reported. The peak 1, therefore, is

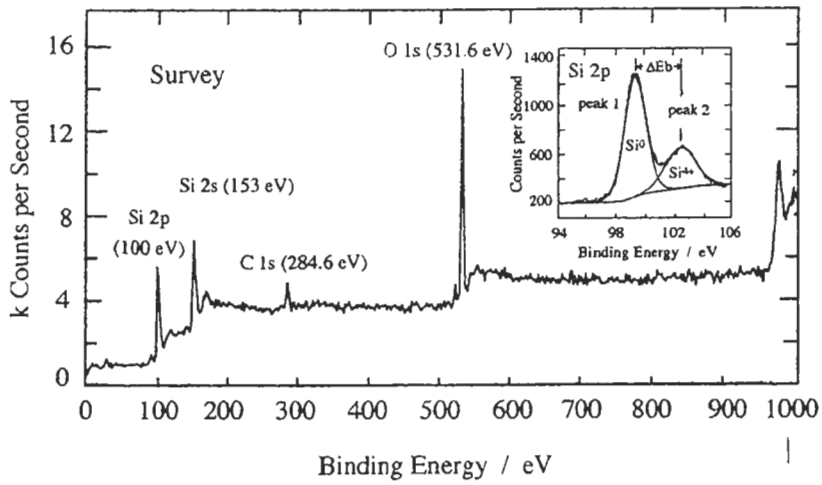

Fig. 8 XPS survey spectrum and high resolution narrow spectrum (inset) for PSL
The PSL was prepared with electrochemical etching ($25Am^{-2}$, 1.8ks) in 35wt% HF aqueous solution.

assigned to the summation of elemental Si and hydrogenated Si in PSL. On the other hand, the peak 2 is assigned to tetravalent Si in SiO_2 film, since the binding energy of peak 2, is close to that of tetravalent Si (103.4eV) in the literature[24]. The binding energy of peaks 1 and 2, their area per cent, PL intensity and crystallinity for the PSL prepared with electrochemical etching and subjected to the surface treatments are listed in Table 1. The area per cent of peak 2 would correspond to the amount of SiO_2 in the PSL. The amount of SiO_2 in PSL increases in the order of electrochemical etching < dip into HF solution < anodic oxidation < dry oxidation < hydrothermal oxidation, suggesting that there is no systematic correlation between amount of SiO_2 and PL peak intensity. Table 1 also suggests that the crystallinity of PSL has no correlation with the PL intensity.

3.3 Correlation between nanostructure, crystallinity, composition and PL properties of PSL

As seen from the above results, the PSL consisting of Si nanoparticles is not the sufficient condition for visible luminescence, although it is the necessary condition. The PSL as prepared with electrochemical etching has a mosaic structure of crystal and amorphous which is independent of electrochemical etching conditions (HF concentration and current density). The PL intensity has a strong correlation with the concentration of SiHx only for the PSL as prepared with electrochemical etching condition. At present, the real distribution of SiH_x in the PSL is unclear because the FT-IR spectra would provide an average information of SiH_x in a certain depth of PSL. The distribution of SiH_x in the PSL is important for the compositional changes due to the subsequent surface treatments. If each Si

Table 1 XPS data for Si 2p binding energy, PL peak intensity, and crystallinity for the PSL subjected to the surface treatments

Sample name	Binding energy of Si 2p (peak 1) / eV	Binding energy of Si 2p (peak 2) / eV	Difference in binding energy, ΔE_b / eV	Peak 1 area (%)	peak 2 area (%)	PL peak intensity, I / a.u.	crystallinity
Electrochemical etching	99.2	102.3	3.1	67	33	not observed	crystal and amorphous
Anodicoxidation	97.7	101.0	3.0	40	60	0.04	amorphous
Dip into HF solution	99.4	102.4	3.3	53	47	0.68	crystal and amorphous
Hydrothermal oxidation	98.9	102.6	3.7	25	75	0.84	amorphous
Dry oxidation	99.0	102.5	3.5	31	69	not observed	crystal and amorphous

nanoparticle is covered with SiH_x layer, the subsequent anodic oxidation, hydrothermal oxidation or dry oxidation would start from SiH_x and proceed with two succesive steps of $SiH_x \rightarrow Si \rightarrow SiO_2$, followed by the final oxidation of elemental Si inside of Si nanoparticles. In contrast, if each Si nanoparticle consist of a mixture of SiH_x and elemental Si, the oxidation of SiH_x and elemental Si would proceed simultaneously. No correlation between crystallinity, composition (concentration of SiH_x or amount of SiO_2) and PL intensity was observed for the PSL subjected to the surface treatments. The following problems will arise as the reasons for no correlation.

(1) The information on amount of SiO_2 obtained from XPS analysis is limited to the uppermost layer of the PSL and does not represent the information of whole depth of the PSL because the escape depth of Si 2p electrons is in the order of several nanometers. The visible PL emits from the region of PSL much deeper than the escape depth of Si 2p electrons. If the amount of SiO_2 is different in depth of PSL, the amount of SiO_2 obtained from the XPS analysis would not correlate with the PL intensity.

(2) The same situationm ay be taken into consideration for correlation between concentration of SiH_x and PL intensity. The average depth ($\approx$0.1μm) of PL emission is less than the FT-IR information depth ($\approx$1μm) of SiH_x because an UV light of 350nm is used as an excitation wavelength for PL emission. The good correlation between concentration of SiH_x and PL intensity for the PSL as prepared with electrochemical etching may suggest the relatively uniform distribution of SiH_x in whole depth of the PSL. On the other hand, no correlation between concentration of SiH_x and PL intensity for the PSL subjected to the surface treatments may be attributed to the oxidation of SiHx depending on the depth of the PSL.

(3) The TED pattern shows only an average crystallinity of the PSL. It is difficult to evaluate separately the crystallinity of each constituent (SiH_x, elemental Si or SiO_2) of PSL from the TED pattern, which would lead apparently no correlation between average crystallinity and PL intensity.

(4) If the PL center is localized in the PSL, it is essentially necessary to evaluate the nanostructure, crystallinity and composition at the center. A scanning near-field optical microscope[25] (SNOM) under development would be powerful tool to determine the local position of PL center.

As seen from the above discussion, we need to examine the distribution of PL center and then evaluate the nanostructure, crystallinity and composition at the PL center.

4. Summary

The results obtained from the present study of PSL subjected to the surface treatments is summarized as follows.

The PL intensity increased with decreasing concentration of SiH_x, only for the PSL as prepared under different electrochemical etching conditions.

The PL intensity was enhanced significantly by HF dip treatment after anodic oxidation or by hydrothermal oxidation in boiling water.

No correlation between nanostructure, crystallinity, composition (SiH_x, elemental Si and SiO_2) and PL intensity was observed for the PSL subjected to the surface treatments. The reason for no correlation was explained in terms of the difference in information depth between FT-IR, XPS and PL emission, or in depth-distribution between each constituent (SiH_x, elemental Si and SiO_2) and PL center.

Acknowledgement

One (Shigyo) of the authours was financially supported by the Sasakawa Scientific Research Grant from the Japan Science Society. The authors are inbebted to Mr. K. Uemura (Nippon Steel Co.) for the donation of p-type Si single crystal wafers and Mr. I. Saeki (Graduate School of Eng., Hokkaido University) for the operation of XPS.

References

1. L. T. Chanham, *Appl. Phys. Lett.*, **57**, 1046 (1990).
2. A. G. Cullis, and L. T. Chanham, *Nature.*, **353**, 335 (1991).
3. V. Lehmann and U. Gosele, *Appl. Phys. Lett.*, **58**, 856 (1991).
4. Qi Zhang and S. C. Bayliss, *J. Appl. Phys.*, **79**, 1351 (1996).
5. P. McCord, S-L. Yau, and A. J. Bard, *Science,* **257**, 68 (1992).
6. M. S. Brandt, H. D. Fuchs, M. Stutzmann, J. Weber and M. Cardona, *Solid State Comm.*, **81**, 307 (1992).
7. K. Shigyo, M. Seo, K. Azumi, H.

Takahashi, M. Al-Odan, and W. H. Smyrl, *Electrochemical Society Proceedings,* **95-8**, 3 (1995).
8. K. Shigyo, M. Seo, K. Azumi, H. Takahashi, M. Al-Odan, and W. H. Smyrl, *J. Surf. Fnish. Soc. Jpn.,* **47**, 157 (1996).
9. K. Shigyo, M. Seo, K. Azumi, and H. Takahashi, *J. Surf. Fnish. Soc. Jpn.,* **47**, 949 (1996).
10. J. C. Vial, A. Bsiesy, F. Gaspard, R. Herino, M. Ligeon, F. Muller, R. Romestain, and R. M. Macfarlane, *Phys. Rev. B,* **45**, 14171 (1992).
11. S. Billat, *J. Electrochem. Soc.,* **143**, 1055 (1996).
12. Y. Kanemitsu, T. Futagi, T. Matsumoto, and H. Mimura, *Phys. Rev. B,* **49**, 14732 (1994).
13. X. Y. Hou, G. Shi, W. Wang, F. L. Zhang, P. H. Huang, and X. Wang, *Appl. Phys. Lett.* **62**, 1097 (1993).
14. Y. Ogata, H. Niki, T. Sakka, and M. Iwasaki, *J. Electrochem. Soc.,* **142**, 195 (1995).
15. C. Tsai, K.-H. Li, and J. C. Campbell, *J. Electronic Materials,* **21**, 589, (1992).
16. J. Rappich and H. J. Lewerenz, *Electrochim. Acta,* **41**, 675 (1996).
17. L. Zhang, J. L. Coffer, D-X. Xu, and R. F. Pinizzotto, *J. Electrochem. Soc.,* **143**, 1390 (1996).
18. H. Bender, S. Verhaverbeke, and M. M. Heyns, *J. Electrochem. Soc.,* **141**, 3130 (1994).
19. T. Takagahara and K. Takeda, *Phys. Rev. B,* **46**, 15578 (1992).
20. St. Frohnhoff, M. Marso, M. G. Berger, M. Thonissen, H. Luth, and H. Munder, *J. Electrochem. Soc.,* **142**, 615 (1995).
21. Y. Suda and N. Koshida, *DENKI KAGAKU,* **63**, 892 (1995).
22. J. Rappich and H. J. Lawerenz, *J. Electrochem. Soc.,* **142**, 1233 (1995).
23. C. D. Wagner, H. A. Six, W. T. Jansen and J. A. Taylor, *Appl. Surf. Sci.,* **9**, 203 (1981).
24. J. A. Taylor, *Appl. Surf. Sci.,* **7**, 168 (1981).
25. S. Jiang, J. Ichihashi, H. Monobe, M. Fujishima, and M. Ohtsu, *Opt. Comm.,* **105** 173 (1994).